hardening coefficient about 1 kg/mm² at the lower strain rate. Figure 1 shows how the over-all screw dislocation density N increased with shear stress in {110}⟨110⟩ at a strain rate of 4.2×10^{-5} sec^{-1}. The crossed bars indicate the maximum deviations in the measured values of N and τ from the average of five equally treated specimens. At higher values of N than about $2\cdot10^6$ cm^{-2} the etch pits could no longer clearly be resolved. Figure 2(a) shows that the measurements are best to be represented within the experimental error by the relation

$$\tau=A(N)^{\frac{1}{2}},\quad A=7.2\cdot10^{-3}\text{ kg/cm}. \tag{1}$$

For each of the four operating slip systems the same law should hold with a coefficient $2A$ instead of A. It is interesting to see that Eq. (1) extrapolates right to the origin so that no additional friction mechanism seems to work at this strain rate besides dislocation interaction (for $\dot\epsilon=8.4\cdot10^{-4}$ sec^{-1}, curve (b), the corresponding curve did, however, extrapolate to a finite friction stress of 22 g/mm²). If one interprets τ in terms of *Taylor's theory* as mean elastic stress of a statistical array of parallel screw dislocations, Eq. (1) is obtained with

$$2A_T=[(C_{11}-C_{12})/4\pi](a/\sqrt{2})\cdot\alpha.$$

The C_{ik} are the elastic constants,[6] and a is the lattice parameter of NaCl at room temperature. Comparison with experiment yields $\alpha=13$. The factor α could arise from the additional influence of edge dislocations not considered in Eq. (1) and/or from the action of groups of (less than) α dislocations. The screw dislocation etch pits rarely showed piled-up arrays. Each pit, measuring several microns in diameter, might correspond to more than one dislocation though. A *forest hardening* mechanism would also result in a relation of the type of Eq. (1) with another meaning of A. It differs from the Taylor mechanism especially in that it should depend stronger on temperature and strain rate. Experimentally, Eq. (1) was found to hold also at the higher strain rate ($8.4\cdot10^{-4}$ sec^{-1}) with almost the same value of A ($7.1\cdot10^{-3}$ kg/cm) [Fig. 2(b)]. It is therefore unlikely that forest hardening accounts for a major part of our observations. Also, the critical shear stress of NaCl at 300°K is about the same as that at 1000°K[7] where the forest ought to be transparent already.

That there is a small thermally activated contribution to plastic flow of NaCl at room temperature can be seen in another type of experiment. If the strain rate is suddenly changed from $\dot\epsilon_1$ to $\dot\epsilon_2$ thermal activation should give a reversible change in flow stress of $\Delta\tau=-[kT/(dU/d\tau_r)]\cdot\ln(\dot\epsilon_2/\dot\epsilon_1)$ if $U(\tau_r)$ is the activation energy of the process and $\tau_r=\tau-A_T\cdot(N)^{\frac{1}{2}}$. In a linear approximation $-dU/d\tau_r$ equals W, the activation volume. Experimentally we found that, contrary to the observation on metals, the flow stress did not change quite *reversibly* with NaCl. The stress increment for an increase of strain rate was always somewhat larger than the decrease in flow stress on the reverse change. Generally the strain rate can alter by changes in the number of dislocations contributing to flow and in their average velocity V:

$$\Delta\dot\epsilon/\dot\epsilon=\Delta N/N+\Delta V/V.$$

We assume the (smaller) *decrease* in flow stress $\Delta\tau$ on lowering the strain rate to be due to a change in dislocation velocity only and this to be controlled by the thermally activated process. From the measured $\Delta\tau\approx10^{-2}$ kg/mm² for an order of magnitude decrease in strain rate we get $W=b^2l=10^{-19}$ cm³ which corresponds to an obstacle spacing l of about 10^{-4} cm.

In conclusion, the flow stress of NaCl seems to depend on the screw dislocation content as expected by theoretical arguments about long range elastic dislocation interaction. This result is similar to conclusions drawn by Seeger and others from experiments on fcc metals and quite unlike the observations on LiF.[2] The reasons for this difference can only be speculated about at present.

We wish to thank Professor J. Gilman for advice during his visit to Göttingen and candidate physicists, Joachim Hesse, Miss H. Siebert, Mrs. B. Rannenberg, and Miss M. Reitz, for assistance in the polishing and counting procedures. The Deutsche Forschungsgemeinschaft has supported this work.

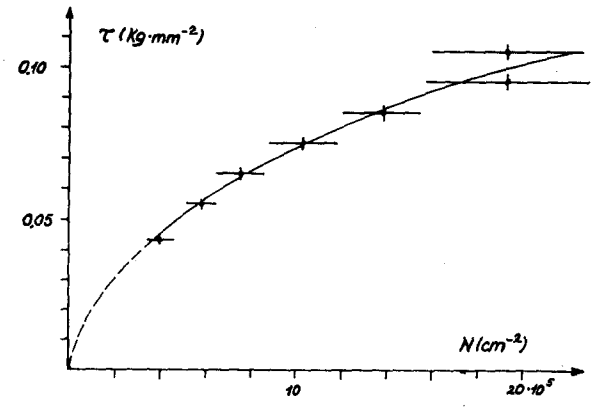

FIG. 1. Flow stress of NaCl vs etch pit density for $\dot\epsilon=4.2\times10^{-5}$ sec^{-1}.

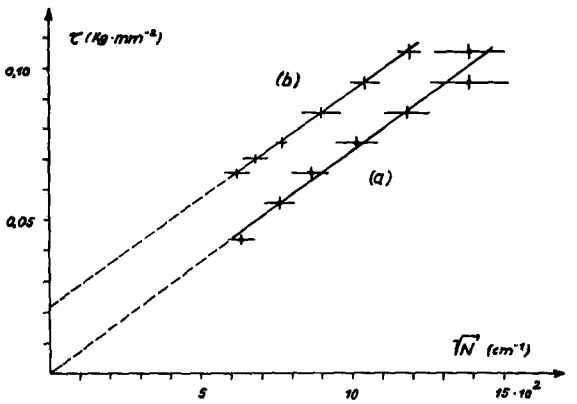

FIG. 2. Illustrating Taylor's law between shear stress and square root of dislocation density. (a) $\dot\epsilon=4.2\times10^{-5}$ sec^{-1}; (b) $\dot\epsilon=8.4\times10^{-4}$ sec^{-1}.

[1] S. Amelinckx, Acta Met. **2**, 848 (1954).
[2] W. G. Johnston and J. J. Gilman, J. Appl. Phys. **30**, 129 (1959), and numerous other papers by the same authors.
[3] We thank Dr. Nitschmann for the selection of specimens.
[4] W. in der Schmitten, Trans. AIME (to be published).
[5] P. R. Moran, J. Appl. Phys. **29**, 1768 (1958).
[6] H. B. Huntington, Progr. Solid State Phys. **7**, 213 (1958).
[7] J. D. Eshelby, C. W. A. Newey, P. L. Pratt, and A. B. Lidiard, Phil. Mag. **3**, 75 (1958).
[8] A. Seeger, *Handbuch der Physik*, edited by S. Flügge [Springer-Verlag, Berlin, Germany, 1955), Vol. VII/2, p. 1.

Quasi-Brillouin Electron Streams

M. H. MILLER
Electron Physics Laboratory, Department of Electrical Engineering, University of Michigan, Ann Arbor, Michigan
(Received April 12, 1961)

THE analysis of rectilinear M-type electron tubes is usually based on a laminar Brillouin flow electron stream model. Because of the peculiarities associated with launching a crossed-field stream, the assumption of laminar flow is somewhat optimistic. One measure of this optimism is the discrepancy between experimental and theoretical stream current densities; in practice, current densities as low as ten percent of the theoretical value are found.

In the stream model derived below the assumption of laminar flow is discarded. The discrepancy noted above is easily explained in terms of nonlaminarity, and other significant results are noted.

The hydrodynamic description of a dc particle flow is given in terms of the following three conservation equations[1]:

$$\nabla\cdot\rho v=0, \tag{1}$$

$$-\eta[\bar{E}+v\times\bar{B}]=(v\cdot\nabla)v+\frac{1}{\rho}\nabla\cdot\rho\bar{\bar{P}}, \tag{2}$$

$$2\eta\Phi=v\cdot v+\langle\bar{u}\cdot\bar{u}\rangle. \tag{3}$$

The average electric field, magnetic field, velocity, and space-charge density associated with the electron velocity distribution in a given volume element are represented by $\bar{E}$, $\bar{B}$, v, and ρ, respectively. The magnitude of the electron charge-to-mass ratio is η, and Φ is the electrostatic potential corresponding to $\bar{E}$. The excess-over-average velocity $\bar{u}$ is the difference between the velocity of a particular electron and the local average velocity v. The enclosures $\langle\ \rangle$ denote the average over the velocity distribution of the enclosed quantity. The symmetrical tensor $\bar{\bar{P}}$ is defined by its elements $\langle u_\alpha u_\beta\rangle$, where α and β form all combinations in pairs of the rectangular coordinates x, y, z.

As written, Eq. (3) is predicated on the assumption that the electron velocity distribution is a distribution in direction only, i.e., all electrons in a given volume element have the same magnitude of velocity. This assumption is justified provided it is acceptable to consider the electrons to leave a unipotential cathode with negligible initial velocities. In the case of an M-type flow this assumption is equivalent to assuming that the predominant cause of turbulence in the dc flow stems from the asymmetry in the gun structure.

Equations (1) through (3) are no full substitute for the Boltzmann transport equation from which they are derived. It is necessary to supplement these equations by one means or another with further information about the electron velocity distribution. The most common additional specification made is that of laminar flow; in this case $\bar{u}$ is identically zero by definition, and the equations reduce to their familiar laminar form. [Equation (3) becomes the result of taking the gradient of Eq. (2).]

For the nonlaminar flow model being derived, additional information about the velocity distribution function is provided indirectly by specifying some of the average properties of the flow. The specifications are made by analogy to laminar Brillouin flow. In essence, what is done is to assume a model, and then to determine the conditions under which the model is consistent with physical laws.

In particular, the stream is assumed to be confined by appropriately oriented electric and magnetic fields so as to flow between planar boundaries $y=a$, b, with $a\leq b$. The average stream velocity is assumed to be

$$v=\Omega y\bar{x}, \tag{4}$$

where Ω is an as yet undetermined constant, and $\bar{x}$ is a x-directed unit vector. The space-charge density is assumed to be constant.

It will be noted that the model is very much like laminar Brillouin flow, except that no constraints have been placed on the magnitudes of v and ρ as yet.

Under the specified conditions, the solution of Eqs. (1) through (3) is straightforward. It is found (with the help of Poisson's equation) that,

$$\langle u_x^2\rangle=\langle u_y^2\rangle=(\omega_p^2-\omega_c^2)(y-a)(y-b)/2, \tag{5}$$

$$\langle u_xu_y\rangle=\langle u_yu_x\rangle=0, \tag{6}$$

$$2\eta\Phi=\omega_c^2y^2+(\omega_p^2-\omega_c^2)(y-a)(y-b), \tag{7}$$

$$\Omega=\omega_c, \tag{8}$$

$$\omega_p^2\leq\omega_c^2. \tag{9}$$

The plasma frequency ω_p and the cyclotron frequency ω_c are defined as usual.

These results are based on the boundary condition that $\bar{u}$, and hence all its averages, is identically zero on the stream boundaries. This requirement follows from the condition that all electrons in a given volume element have the same magnitude of velocity, and because there is no normal (y-directed) velocity component of any electron on the stream boundaries. Since all electrons have the same magnitude and direction of velocity on the stream boundaries, the excess-over-average velocity of any electron is zero.

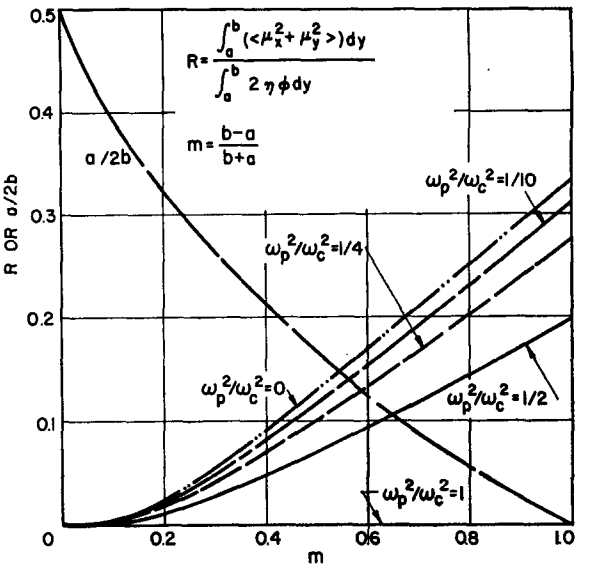

FIG. 1. Comparison between quasi-Brillouin and laminar Brillouin flows.

It might be noted that this model can be derived by requiring the pressure tensor $\bar{\bar{P}}$ to be diagonal, with equal diagonal elements, i.e., "hydrostatic."

It is interesting to note that there is no choice as to the value of the velocity slip Ω; it must be equal to ω_c. At the same time, the plasma frequency can be less than the cyclotron frequency. This situation is quite different from the laminar Brillouin model where $\omega_p^2=\omega_c^2$, or from the partially neutralized model where the effective plasma frequency can be less than the cyclotron frequency, but the velocity slip is ω_p^2/ω_c.

The requirement of Eq. (9) follows, in the present model, from considering Eq. (5) in the light of the fact that $\langle u_x^2\rangle$ and $\langle u_y^2\rangle$ are inherently positive quantities. When the equality applies, the nonlaminar model reduces to laminar Brillouin flow. For this reason the nonlaminar model is referred to as "quasi-Brillouin" flow.

As an index of comparison between a quasi-Brillouin stream and a laminar flow of the same geometry, use can be made of the fraction, denoted by R, of the total stream energy involved in the excess-over-average motion;

$$\frac{1}{R}=\frac{\int_a^b 2\eta\Phi dy}{\int_a^b(\langle u_x^2\rangle+\langle u_y^2\rangle)dy}=1+\frac{2}{1-(\omega_p^2/\omega_c^2)}\frac{m^2+3}{4m^2}, \tag{10}$$

where m is a convenient geometric parameter,

$$m=(b-a)/(b+a). \tag{11}$$

Figure 1 is a graph of R as a function of m, for various values of ω_p^2/ω_c^2. Also drawn for convenience is a conversion curve relating m and a/b.

For a nominal value of $m=1/3(b=2a)$, a value of R equal to only 0.04 corresponds to a space-charge density (and current density) which is 0.4 that of a laminar flow of the same geometry. Increasing R to 0.06 reduces the space-charge density to 0.1 of the laminar Brillouin value.

It is, of course, questionable whether the quasi-Brillouin flow model is any more realistic than the laminar flow model. However, the nonlaminar flow model has the advantage of recognizing the existence of nonlaminar motion. It thus stands some chance to profit from the philosophy that the general characteristics of an electron stream are not critically dependent on the exact details

of the flow. One particular case where this might bear fruit is the analysis of the rf properties of a crossed-field flow.

[1] S. Chapman and T. G. Cowling, *Mathematical Theory of Nonuniform Gases* (Cambridge University Press, New York, 1952).

Liquidlike Layers on Ice

H. H. G. JELLINEK
Department of Chemistry, Essex College, Assumption University of Windsor, Windsor, Ontario, Canada
(Received December 7, 1960)

RECENTLY Kingery[1] described experiments on the growing together of ice spheres. The experiments seem to indicate that the growth process is due to surface diffusion. However, a very high value was found for the effective surface diffusion coefficient, "several orders of magnitude larger than is to be expected." Also the energy of activation for this diffusion process was found to be rather large.

Faraday[2] explained his experiments "on regelation" by the assumption of a liquidlike layer on ice below its melting point. This view was opposed by Thomson[3] and Thomson[4] who maintained that regelation is due to pressure melting. However, more recently, the liquidlike layer theory was revived by Weyl[5] on theoretical grounds and by Nakaya and Matsumoto[6] and Jensen,[7] who showed that ice spheres, once having touched one another, behaved on separation as if a liquidlike layer were present on the ice surfaces. Jensen was able to show that, in water vapor saturated atmospheres, indication of a liquidlike layer persisted down to $-25°C$, whereas in a dry atmosphere the liquidlike layer seemed to be absent at temperatures lower than $-3°C$.

Kingery attempts to explain the growth of a neck between two ice spheres by assuming high surface mobility of molecules and tends to the view that a liquidlike layer is not necessary to account for his results. The following quotation from his paper is noteworthy: "Nakaya and Weyl have interpreted observations of the adhesion between ice particles and regelation phenomena in terms of a mobile "liquid like" surface structure. If this is considered as a layer of several atomic dimensions having appreciable atomic mobility, the experimental results would be as expected here; this would provide a mechanism for rapid surface diffusion. At the same time, there is nothing in the present experimental results that is not adequately explained on the basis of a surface layer one or a few molecules in any case." He then goes on to discard the liquidlike layer concept on the grounds that "it is difficult to accept the fact that we have a liquid layer at a temperature some 25° below the melting point."

It should be pointed out, however, that his view and the liquidlike layer theory are very close and differ only by degree, i.e., thickness of the mobile layer. Further, the experiments by Jensen with spheres in a saturated atmosphere show that a liquidlike layer seems to exist down to $-25°C$. There might also well be a break in the curve of temperature dependence (Fig. 5, Kingery[1]) at a temperature in the neighborhood of $-9°C$. The present writer has made an extensive investigation of the adhesive properties of ice.[8] Tensile and shear experiments with ice sandwiched between disks of stainless steel, various polymers, and quartz optical flats were carried out. The shear experiments with highly polished metal and optically flat quartz surfaces showed distinct characteristics of sliding similar to those which one should except from a liquidlike layer between ice and the respective surface, whereas the tensile experiments led only to cohesive breaks in the ice. These results seem only to be comprehensible on the basis of the assumption of a liquidlike layer not only for the ice/air interface but also for the ice/metal, ice/polymer, and ice/quartz interfaces. The tensile experiments lead to cohesive breaks because of the action of surface tension forces inherent in the liquidlike layer sandwiched between the ice and the respective metal, polymer, or quartz surfaces. The ice "adheres" to the respective surfaces due to the pressure difference across the curved liquidlike layer/air interface, governed by the equation $\Delta p=\gamma(1/r_1+1/r_2)$, where Δp is the pressure difference, γ the interfacial tension (liquidlike layer/air), and r_1 and r_2 the principal radii; for a liquidlike layer of thickness 2×10^{-6} cm or 70 water molecules and $\gamma=76.4$ d/cm (r_2 being large), one obtains for $\Delta p=70$ kg/cm^2, appreciably above the tensile strength of bulk ice (12 to 15 kg/cm^2), although it should be noted that the tensile strength of ice increases with decreasing volume.[9] In contrast, shear experiments show that only very small stresses are needed to produce sliding eventually leading to an adhesive break. Reasonable estimates of the viscosity and thickness of the liquidlike layer could be made from the experiments, assuming the liquid to be Newtonian as a first approximation. It must be realized that such layers will probably show a continuous transition from the crystalline solid to a fairly viscous liquid and will also be dependent on the nature of the interface (metal, polymer, quartz). Estimates of the thickness and viscosity of the layers deduced from experiments at $-4.5°C$ ranged from about 10^{-5} to 10^{-6} cm and viscosities from 70 to 700 poises for ice/stainless steel and 15 to 150 poises for ice/quartz. Shear experiments with thin water films (0.2 to 1 μ) between optically flat glass plates[10] showed very similar characteristics to those obtained from the experiments with ice. Thus it appears that Kingery's results, considered in conjunction with the experiments on adhesion of ice, rather support the liquidlike layer theory.

It may also be remarked that work by Hori[11] on the properties of thin water films sandwiched between glass and quartz plates revealed abnormal vapor pressures and freezing points at low temperatures even after taking into consideration interfacial free energies and curvatures of surfaces. Thus, for instance, films 1.3×10^{-4} cm thick placed between glass plates did not freeze even at $-96°C$.

The investigations on ice adhesion,[8] tensile strength of ice,[9] and frictional properties of thin water films[10] were carried out at the U. S. Army Snow Ice and Permafrost Research Establishment, Corps of Engineers, Wilmette, Illinois.

[1] W. D. Kingery, J. Appl. Phys. **31**, 833 (1960).
[2] M. Faraday, Phil. Mag., 4th Ser. **17**, 162 (1859); Proc. Roy. Soc. (London) **10**, 440 (1860); see also J. Tyndall, *ibid.* **9**, 141 (1858).
[3] J. Thomson, Proc. Roy. Soc. (London), **A10**, 152 (1859); **11**, 198, 473, (1861).
[4] W. Thomson, Proc. Roy. Soc. (London) **A9**, 761 (1858).
[5] W. A. Weyl, J. Colloid Sci. **6**, 389 (1951).
[6] U. Nakaya and A. Matsumoto, J. Colloid Sci. **9**, 41 (1954), also U. S. Army Snow Ice and Permafrost Research Establishment, Corps of Engineers, Research Paper 4 (1953).
[7] D. C. Jensen, M. S. thesis, Pennsylvania State University (1956).
[8] H. H. G. Jellinek, Adhesive Properties of Ice, U. S. Army Snow Ice and Permafrost Research Establishment, Corps of Engineers, Research Report 38 (1957), and Research Report 62 (1960). See also J. Colloid Sci. **14**, 268 (1959).
[9] H. H. G. Jellinek, Proc. Phys. Soc. (London) **71**, 797 (1958), also U. S. Army Snow Ice and Permafrost Research Establishment, Corps of Engineers, Research Report 23 (1957).
[10] H. H. G. Jellinek, U. S. Army Snow Ice and Permafrost Research Establishment, Corps of Engineers, Special Report 37 (1960).
[11] T. Hori, U. S. Army Snow Ice and Permafrost Research Establishment, Corps of Engineers, Translation 62, also Teion Kagaku Butsuri Hen **A15**, 34 (1956).

Available Power from a Nonideal Thermal Source*

PAUL PENFIELD, JR.
Department of Electrical Engineering and Research Laboratory of Electronics, Massachusetts Institute of Technology, Cambridge 39, Massachusetts
(Received April 28, 1961)

MANY analyses of heat engines, including thermoelectric generators, are based on the availability of heat reservoirs with which heat may be exhanged reversibly. An exception is the analysis of Gray,[1] who discusses thermoelectric generators and their efficiency optimization, when they are connected to a nonideal heat source consisting of two heat reservoirs, with finite thermal resistances separating the reservoirs from the thermocouple. Gray's device is a special case of the device pictured in